Proceedings of the 2018 IEEE
International Conference on Robotics and Biomimetics
December 12-15, 2018, Kuala Lumpur, Malaysia

Force Control of Flexible Integrated Joint Based on Model-free Adaptive Control

Yingli Li, Yiwen Zhao, Kai Li, Zheng Wang and Xingang Zhao

Abstract— **The flexible integrated joint (FIJ) is a key part of the collaborative robots, which has the characteristics of lightweight and highly integration. The force control is pivotal for achieving compliant interactions with environments and humans, such as impendence control and force tracking control. However, the controller design for force control of the flexible joint is a challenging issue with unmodeled uncertainties, nonlinear friction, time-varying load and other disturbances forced by environments in general. In this paper, a control scheme based on model-free adaptive control (MFAC) was developed for the force control of the FIJ. First, the model of the FIJ was transformed into a virtual dynamic linearization data model by a dynamic linearization approach. Second, a MFAC algorithm was designed for force control of the FIJ, including its corresponding pseudo gradient estimating algorithm and pseudo gradient resetting algorithm. To evaluate the performance of the proposed method, the experiments including zero force tracking and step force tracking were carried out in this research. The experimental results show that the developed control approach can get a high performance as the dynamical parameters of the FIJ are time-varying and uncertain.**

I. Introduction

Extensive use of flexible manipulators in various robotic applications has made it as one of the research interests for many researchers over the last few decades [1]. In recent years, the design of light-weight robots with a high load/weight ratio is the trend in the research of robots, especially in the fields of space, surgical and service robotics. A major problem for the implementation of lightweight robot is the inherent flexibility introduced into the robot joints [2]. The flexibility of the robotic joints is mainly caused by the gear inherent elasticity in harmonic drive transmission and elasticity of the torque sensor's strain gauge. The experimental results showed that the flexibility of the joints should be taken into account in both modeling and controller design process if high performance was expected [3]. Compared to traditional manipulators, the flexible manipulators need to have an additional function of sensitive force control, such as compliance and safe interaction control. The force control of the flexible joints is the basis of compliant interactions with environment and humans, which has been widely studied for many years. A unified passivity-based control framework incorporated with an inner torque feedback loop was proposed to solve the problem of position, torque and impedance control of flexible robotic joints in [2]. Mbede and Mvogo Ahanda designed an exponential tracking controller using backstepping approach to realize the flexibility of joints in an electrically driven robot in [4]. A new control technique based on the disturbance observer is proposed to suppress torsional vibration [5]. In order to improve performance of force control, Montgomery *et al.* analyzed the range of the model uncertainty and proposed a decentralized approach which was realized by leveraging disturbance observers in the robot's joint-level torque controllers [6]. As mentioned above, the controller design of most force control methods is based on the model of plant. Moreover, disturbance observer introduced in the force control can only reject disturbance at a limited level. Before designing the controller, the dynamic model of the joint has been already known or the model structure is known and model parameters can be accurately obtained by online estimation [7]. However, it is well known that the nonlinearity commonly exists in practical systems and unmodeled dynamics are also inevitable. The model of the inner control loop (torque control loop) includes complex mechanical dynamics, nonlinear friction, harmonic drive vibration and other unknown disturbances from environments. It is difficult or even impossible to build an accurate model for the plant. Therefore, the model-based control methods are greatly limited in the practical force control of the flexible joint.

The model-free adaptive control (MFAC) method is a typical data-driven control method that the I/O measurement data of the controlled plant is merely used to design the controller, without explicitly or implicitly using the plant structure or dynamics information of the controlled plant [8], [9]. This control method is suitable for the linear or nonlinear plant. The modeling process, the unmodeled dynamics, the time-varying parameters and the theoretical assumptions on the dynamics of the plant do not exist since the MFAC method does not require a model of the plant in the controller design process [7]. The MFAC approach can guarantee the bounded-input bounded-output stability and the tracking error convergence. However, when the convergence speed of the tracking error is slow, a reset algorithm is needed to make parameter estimation algorithm have a stronger ability in tracking time-varying parameter [7]. Because the MFAC method is based on a dynamically linearized data model of the controlled system which is estimated by I/O measurement data,

*This work is supported by National Key Laboratory of Robotics Program of China (Nos. Y7C120H101) and Program of Institutes for Robotics and Intelligent Manufacturing, Chinese Academy of Sciences (Nos. C2016001).

Yingli Li and Kai Li are with the State Key Laboratory of Robotics, Shenyang Institute of Automation, Chinese Academy of Sciences, with Institutes for Robotics and Intelligent Manufacturing, Chinese Academy of Sciences, Shenyang 110016, China and also with the University of the Chinese Academy of Sciences, Beijing 100049, China (e-mail: liyingli@sia.cn)

Yiwen Zhao, Zheng Wang and Xingang Zhao are all with the State Key Laboratory of Robotics, Shenyang Institute of Automation, Chinese Academy of Sciences, and also with Institutes for Robotics and Intelligent Manufacturing, Chinese Academy of Sciences, Shenyang 110016, China

978-1-7281-0377-8/18/$31.00 © 2018 IEEE

it could essentially overcome the issue of unmodeled dynamics and robustness. The MFAC method can be applied to the areas where the model is difficult to build precisely, such as motion control system, networked nonlinear system and chemical control system [10], [11].

In this paper, a force controller based on the MFAC control method was designed for the FIJ. The main motivation of this work was to improve the force control performance of JIF by using the MFAC method. The contents of this paper are organized as follows: Section II describes the platform of the research in detail. The nonlinear autoregressive moving average with exogenous input (NARMAX) model of the plant is obtained in section III based on dynamics analysis and transfer function. Then, the dynamical linearization data model is obtained by a dynamic linearization approach and the MFAC controller is designed in Section IV. Section V conducts some experiments with the proposed method, including zero force tracking and step force tracking experiments. After that, the results are listed out and analyzed. The last section makes a brief summary of this paper and our future work.

II. Platform

The test platform fixed on the calibration table is designed as Fig. 1. The hardware structure of the test system consists of four sub-systems, including the FIJ system, load adjustment system, motor driver system and on-board control system (Embedded PC).

The load adjustment system is used to change the load inertia by adjusting the number of weight plates. The motor driver system mainly includes a motor driver and the circuit board used for power management and sensor data acquisition. The motor driver is G-TWI 10/100 EE series provided by the ELMO Corporation. The control application runs on the Embedded PC which communicates the data with the motor driver system in real time through the EtherCAT bus.

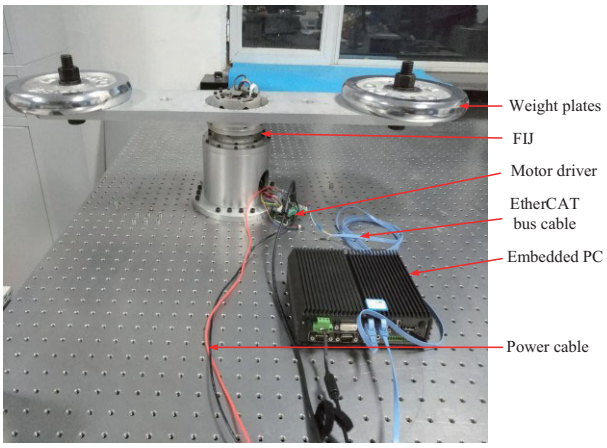

Fig. 1. Sketch of the joint test platform

As shown in Fig. 2, The FIJ integrates sensors and mechanical components that include incremental encoder to measure the position of motor, absolute encoder to measure the position of the output flange, torque sensor to measure the torque between the soft wheel and the output flange, permanent magnet synchronous motor (PMSM), harmonic drive, brake, connecting shaft, and output flange. The basic parameters of the FIJ system are listed in TABLE I. The motor utilized in the FIJ is MF0060008 series frameless brushless torque motor. The absolute encoder is MRAD01 series provided by RENISHAW.

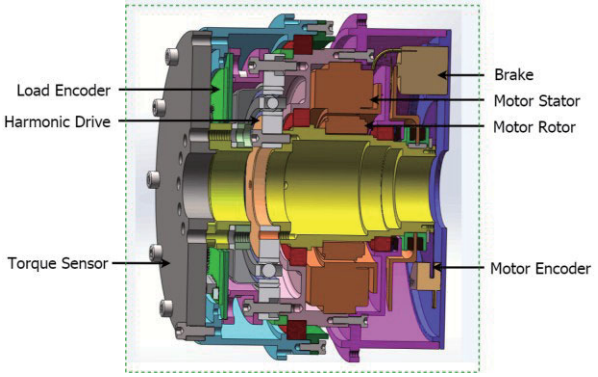

Fig. 2. Sketch of FIJ system

TABLE I
PARAMETERS OF THE FIJ

Weight	Stiffness	Rated Torque	Max Torque	Max Velocity
2.5 kg	34000 Nm/rad	55 Nm	104 Nm	2.1 rad/s

III. Dynamic Model Analysis

We simplify the FIJ model as a spring-damper system shown in Fig. 3. Therefore, the model for the entire joint based on [12] is described as:

$$\begin{aligned} J_l \ddot{\theta}_l + D_l \dot{\theta}_l &= \tau + \tau_{ext} + g(\theta_l) \\ J_m \ddot{\theta}_m + D_m \dot{\theta}_m + \frac{\tau}{N} &= \tau_m \\ \tau &= K(\frac{\theta_m}{N} - \theta_l) \end{aligned} \tag{1}$$

where J_m is the symmetric positive-definite term that represents the motor inertia; N=160 is the reduction ratio between motor side and load side through the harmonic drive; $J_l > 0$ is the load inertia term; D_m is the motor damping term; D_l is the load damping term; θ_m and θ_l are, respectively, the motor position and the load position; $g(\theta_l)$ denotes the gravitational torque; K is the stiffness of virtual spring which is contributed by the torque sensor and harmonic drive; τ_m denotes the output torque of the motor; τ_{ext} is the external torque applied by the environment which is time-varying and uncertain; τ is the deformation torque of virtual spring.

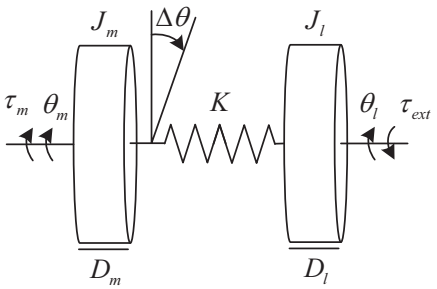

Fig. 3. Spring-damper system

The block diagram of the system control is shown in Fig. 4 which includes the plant, PPD estimator and the MFAC controller. The part which is circled by a green box is the plant corresponding to the dynamic system (1). τ_d is the desired input of the system. τ_m and τ are, respectively, the input and output of the plant. The transfer function of nominal model is built at first, and then convert it to nonlinear autoregressive moving average with exogenous input (NARMAX) model [13].

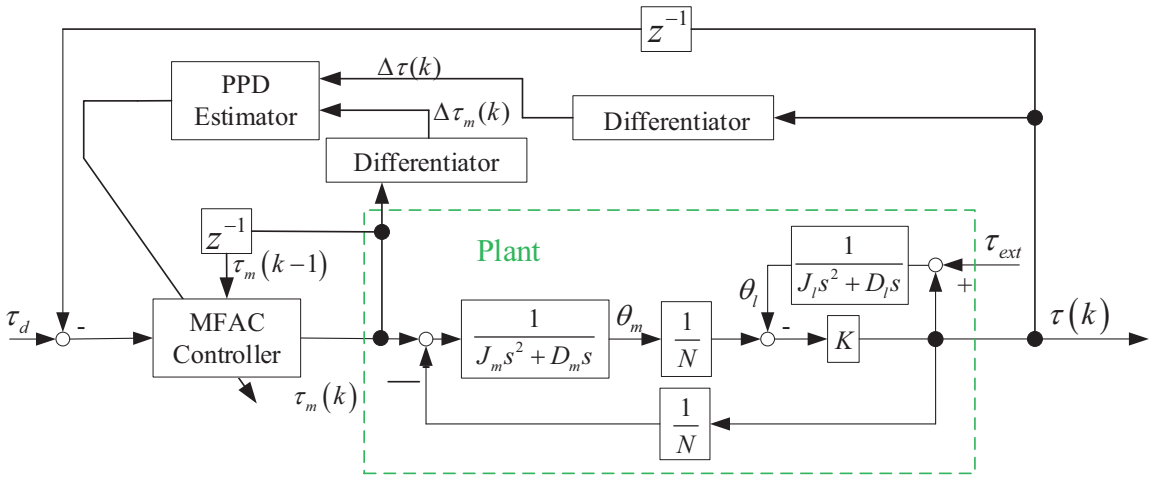

Fig. 4. Block diagram of system control

The transfer function of the plant is

$$\frac{\tau(s)}{\tau_m(s)} = \frac{\alpha(s)}{N} \cdot \frac{1}{J_m s^2 + D_m s + \frac{\alpha(s)}{N^2}} \tag{2}$$

$$\alpha(s) = \frac{K(J_l s^2 + D_l s)}{J_l s^2 + D_l s + K}$$

$$\frac{\tau(s)}{\tau_m(s)} = \frac{b_2 s^2 + b_1 s}{a_4 s^4 + a_3 s^3 + a_2 s^2 + a_1 s}$$

where

$$\begin{aligned} a_4 &= N^2 J_m J_l \\ a_3 &= N^2(J_m D_l + J_l D_m) \\ a_2 &= N^2(K J_m + D_l D_m) + K J_l \\ a_1 &= K(D_l + N^2 D_m) \\ b_2 &= NKJ_l \\ b_1 &= NKD_l \end{aligned} \tag{3}$$

Assume the input of the discrete-time system is $u(k) = \tau_m(k)$ at the k-th moment. The NARMAX model about system (3) is as the following:

$$\begin{aligned} \tau(k+1) = f(&\tau(k), \tau(k-1), ..., \tau(k-4), \\ &u(k), u(k-1), u(k-2)) \end{aligned} \tag{4}$$

where $\tau(k) \in R$ and $u(k) \in R$ are the system output and control input, respectively; Due to external uncertain load, nonlinear friction and torque transmission fluctuation of harmonic drive, $f(.): R^8 \to R$ is the unknown nonlinear transformed form of the force control for the FIJ system which includes time-varying parameters.

IV. Controller Design

A. MFAC Dynamical Linearization

For system (4), vector $\mathbf{H}_{5,3}(\mathrm{k}) \in \mathbf{R}^8$ consists of all inputs within the sliding time window $[k-2, k]$ and all outputs within the sliding time window $[k-4, k]$, as follows (5):

$$\mathbf{H}_{5,3}(k) = \begin{bmatrix} \tau(k), \tau(k-1), ..., \tau(k-4), \\ u(k), u(k-1), u(k-2) \end{bmatrix}^T \tag{5}$$

$\mathbf{H}_{5,3}(k) = \mathbf{0}_8$ for $k \le 0$, $\mathbf{0}_8$ is zero vector whose length is eight.

The following three assumptions are first made [7].

Assumption 1: The system (4) is input and output controllable and measurable, i.e., there is a consistent bounded and feasible input $u(k)$ such that the output $\tau(k)$ tends to the desired output $\tau^*(k)$.

Assumption 2: The partial derivative of $f(.)$ with respect to $u(k)$ and $\tau(k)$ is continuous.

Assumption 3: The system (4) is generalized Lipschitz, i.e., $|\Delta\tau(k+1)| \le b\|\Delta\mathbf{H}_{5,3}(k)\|$ for any k

$$\Delta\mathbf{H}_{5,3}(k) = [\Delta\tau(k), ..., \Delta\tau(k-4), \Delta u(k), ..., \Delta u(k-2)]$$

$$\Delta\mathbf{H}_{5,3}(k) \ne 0$$

where b is a positive constant.

Remark 1: The generalized Lipschitz condition in Assumption 3 imposes an upper bound on the change rate of the system output driven by the change of the control input. From an energy viewpoint, it means that the energy change inside a practical system cannot go to infinity if the energy change of the control input is at a finite level [14]. In practical applications, many practical motion control systems and physical processed satisfy such a property.

Theorem 1: If Assumptions 1 and 2 are satisfied, when $\left\|\Delta H_{5,3}\right\| \neq 0$, there exists a time-varying vector $\boldsymbol{\varphi}_{f,5,3}(k) \in \mathbf{R}^8$, called pseudo gradient (PG), such that system (4) can be converted into the following equivalent dynamic linearization data model [15]:

$$\Delta\tau(k+1) = \boldsymbol{\varphi}_{f,5,3}^T \Delta\mathbf{H}_{5,3}(k) \tag{6}$$

where $\boldsymbol{\varphi}_{f,5,3}(k) = [\varphi_1(k), ...\varphi_8(k)]^T \in R^8$, and $\left\|\boldsymbol{\varphi}_{f,5,3}(k)\right\| \leq b$ is bounded for any k.

The proof of Theorem 1 has been given in [16].

According to the Theorem 1, the dynamic linear model for the system (4) is given as follows:

$$\tau(k+1) = \tau(k) + \boldsymbol{\varphi}_{f,5,3}^T(k)\Delta\mathbf{H}_{5,3}(k) \tag{7}$$

B. Controller Design

Consider the following control input criteria function:

$$J(u(k)) = \left|\tau^*(k+1) - \tau(k+1)\right|^2 + \lambda\left|u(k) - u(k-1)\right|^2 \tag{8}$$

where $\lambda > 0$ denotes the weight factor, the first term is introduced to make the output of the system consistent with the desired output, the second term is the regular term which penalizes big input change to reduce the input energy and oscillations.

Combine the equation (7) and (8), then we get the $u(k)$:

$$\begin{aligned} u(k) = u(k-1) &+ \frac{\rho_6\hat{\varphi}_6(k)(\tau^*(k+1) - \tau(k))}{\lambda + \left|\hat{\varphi}_6(k)\right|^2} \\ &- \frac{\hat{\varphi}_6(k)\sum_{i=1}^{5}\rho_i\hat{\varphi}_i(k)\Delta\tau(k-i+1)}{\lambda + \left|\hat{\varphi}_6(k)\right|^2} \\ &- \frac{\hat{\varphi}_6(k)\sum_{i=7}^{8}\rho_i\hat{\varphi}_i(k)\Delta u(k-i+1)}{\lambda + \left|\hat{\varphi}_6(k)\right|^2} \end{aligned} \tag{9}$$

where $\varphi_i(k)$ is the i-th element of the time-varying parameter vector $\boldsymbol{\varphi}_{f,5,3}(k)$, in order to increase the flexibility of the control algorithm, step factor $\rho_i \in (0,1],\ i = 1,2,...,8$ is introduced.

In order to get the control input $u(k)$ by equation (9), we need to know the value of PG, but the model of the system (4) is unknown and the PG is time-varying. We can utilize the I/O data to estimate the value of the PG online.

Consider the following PG estimation criteria function:

$$\begin{aligned} J(\boldsymbol{\varphi}_{f,5,3}(k)) = &\left|\tau(k) - \tau(k\text{-}1) - \boldsymbol{\varphi}_{f,5,3}^T(k)\Delta\mathbf{H}_{5,3}(k-1)\right|^2 \\ &+ \mu\left\|\boldsymbol{\varphi}_{f,5,3}(k) - \hat{\boldsymbol{\varphi}}_{f,5,3}(k-1)\right\|^2 \end{aligned} \tag{10}$$

where $\mu > 0$ is weight factor.

For equation (10), we get the estimation value of PG by finding the extreme value.

$$\begin{aligned} &\boldsymbol{\varphi}_{f,5,3}(k) = \boldsymbol{\varphi}_{f,5,3}(k-1) + \\ &\frac{\eta\Delta\mathbf{H}_{5,3}(k-1)(\tau(k) - \tau(k-1) - \boldsymbol{\varphi}^T_{f,5,3}(k-1)\Delta\mathbf{H}_{5,3}(k-1))}{\mu + \left\|\Delta\mathbf{H}_{5,3}(k-1)\right\|^2}, \end{aligned} \tag{11}$$

In order to increase the flexibility of the control algorithm, step factor $\eta \in (0,2]$ is introduced. $\boldsymbol{\varphi}_{f,5,3}(k)$ is the estimation value of $\boldsymbol{\varphi}_{f,5,3}(k)$.

In order to make the PG parameter estimation algorithm have a stronger ability in tracking the time-varying parameters, a reset mechanism for PG is taken as follows:

$$\begin{aligned} &\boldsymbol{\varphi}_{f,5,3}(k) = \boldsymbol{\varphi}_{f,5,3}(1) \\ &if: \left\|\boldsymbol{\varphi}_{f,5,3}(k)\right\| \leq \varepsilon \text{ or } \left\|\Delta\mathbf{H}_{5,3}(k-1)\right\| \leq \varepsilon \\ &\quad \text{or } sign(\varphi_6(k)) \neq sign(\varphi_6(1)) \end{aligned} \tag{12}$$

where ε is a little positive value and $\boldsymbol{\varphi}_{f,5,3}(1)$ is the initial value of $\boldsymbol{\varphi}_{f,5,3}(k)$.

The control scheme consists of equation (11), (12), (9). The stability of the control algorithm is strictly mathematical proof in [16].

V. Experiment Setup and Results Analysis

A. Experiment Setup

Experiments have been performed in the FIJ platform that is shown in Fig. 1.

In order to compare the control performance of two kinds of controller, the pendulum device (as shown in Fig. 5) is designed, which is composed of a support frame and a rubber weight connected at the end of rope. When the disturbance is applied to the system, the weight drops from the horizontal position (0 degree) to the vertical position (90 degree) to hit the end of load adjustment system. This ensures that the same amount of disturbance is applied to different experiments as much as possible.

In order to compare the tracking performance of the different control methods quantitatively, the root mean square error (RMSE) index is defined by [17] :

$$\mathrm{RMSE}(.)=\sqrt{\frac{1}{N}\sum_{i=1}^{N}|e_i|^2} \tag{13}$$

where N is the total number of sampling points and e_i is the error between the actual torque and the reference torque at the i-th sampling moment.

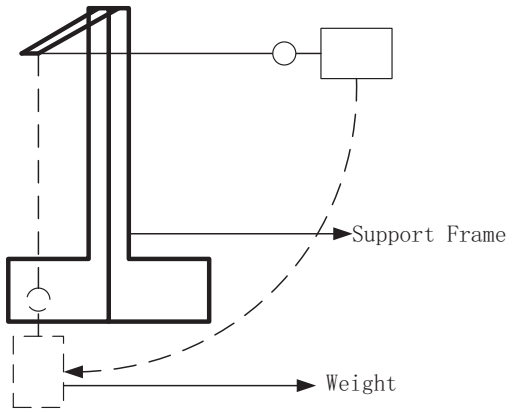

Fig. 5. Device of applying disturbance

B. Results Analysis

For the force control task of the FIJ, it is compared with the incremental PID and MFAC control method. The control period is 1 ms. The incremental PID controller is given as follows:

$$\begin{aligned} &\mathrm{e}(k)=\tau_d(k)-\tau(k)\\ &\Delta u(k)=K_p(\mathrm{e}(k)-\mathrm{e}(k-1))+K_i\,\mathrm{e}(k)+\\ &\qquad K_d\left(\mathrm{e}(k)+\mathrm{e}(k\text{-}2)-2\,\mathrm{e}(k\text{-}1)\right)\\ &u(k)=u(k-1)+\Delta u(k) \end{aligned} \tag{14}$$

The output of controller $u(k)$ is sent to the motor driver by EtherCAT bus at every control period. The optimal parameters for PID control method are obtained by hypothetical model analysis and a large number of experimental testing, i.e.

$$K_p=40, K_i=1, K_d=0.05 \tag{15}$$

Because the force sensor is noisy, the differential parameter is relatively small.

For MFAC control scheme, the parameters of the formula (11), (12), (9) are given as follows:

$$\begin{aligned} &\eta=1.8,\ \ \mu=1,\ \lambda=0.001\\ &\rho_i=0.6, i=\{1,\ldots,8\}\\ &\hat{\boldsymbol{\varphi}}_{f,5,3}(1)=[0.002,0.002,0.002,0.002,\\ &\qquad 0.002,0.002,0.002,0.002] \end{aligned} \tag{16}$$

1) Torque control with zero reference signal

The direct teaching by hand improves robot deployment efficiency and flexibility. For a single joint, in order to accomplish this task, the torque between the motor side and the output flange needs to be controlled to zero as much as possible. The direct teaching experiment for a single joint was conducted, i.e. the desired torque τ_d is set zero.

We applied three different disturbances to the FIJ system using the device in Fig. 3 for two experiments which was controlled by PID and MFAC method, respectively. The tracking performance, the absolute value of error and the performance comparison of the two kinds of methods are shown in Fig. 6, Fig. 7 and Table II, respectively.

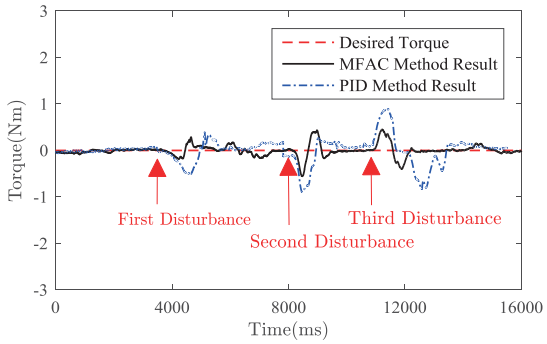

Fig. 6. Tracking performance of two methods

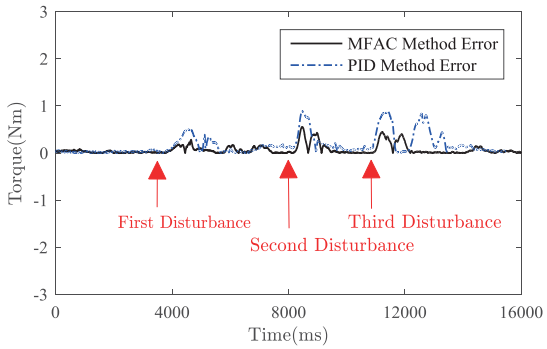

Fig. 7. Absolute value of error of two methods

TABLE II
PERFORMANCE COMPARISON OF TWO METHODS

Item	RMSE	Max Error	Max Stead Error
MFAC	0.1239 Nm	0.4525 Nm	0.02 Nm
PID	0.2761 Nm	0.8881 Nm	0.05 Nm

As can be seen from Fig. 6 and Fig. 7, when the disturbance is small, the tracking effect is relatively good for PID control method. However, when the disturbance is big, the tracking performance is poor and settling time is longer (in the third disturbance process, max error is 0.8 Nm and setting time is 3s). Because the parameters of PID control method is fixed, it does not adapt well to the situation where the model or disturbance is changing large-scale. MFAC control method estimates the PPD of the system online and calculates the corresponding control rate. It is more adaptable to the changes in model and disturbance (max error is 0.45 Nm and setting time is 1s).

2) Torque control with step reference signal

In order to make sure the validation of the MFAC method, a further torque control experiment with step reference signal whose amplitude is 0.2 Nm is conducted at 15s from the

beginning of the control, and the according experimental results are demonstrated in Fig. 8, Fig. 9 and TABLE III.

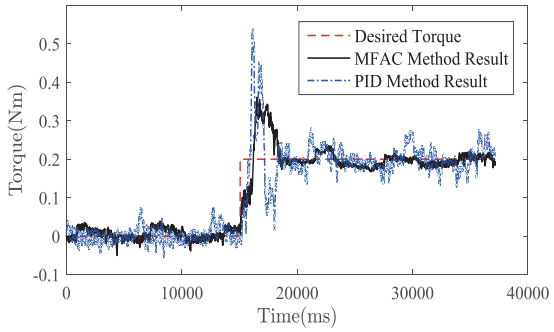

Fig. 8. Tracking performance of two methods

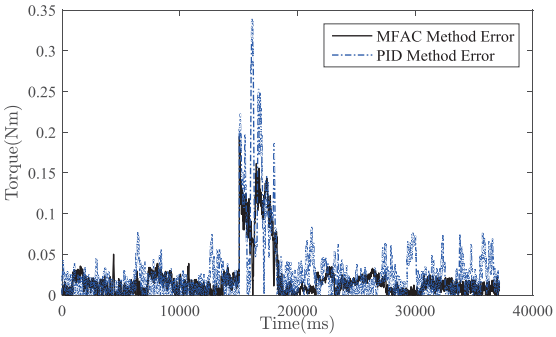

Fig. 9. Absolute value of error of two methods

TABLE III
PERFORMANCE COMPARISON OF TWO METHODS

Item	RMSE	Overshoot	Max Stead Error
MFAC	0.0339 Nm	0.1615 Nm	0.035 Nm
PID	0.0495 Nm	0.3395 Nm	0.085 Nm

From Fig. 8 and Fig. 9, we can see that the MFAC control method has a smaller overshoot (from 0.3395 Nm to 0.1615 Nm) and fluctuation compared with the PID control method.

From the results of experiment 1) and 2), we can see that MFAC method is more adaptable while the dynamical parameters of the FIJ are time-varying and uncertain.

VI. CONCLUSION

In this paper, a control scheme based on MFAC was designed for force control of the FIJ, which estimated the PPD reflecting the system characteristics and improved the performance of the force control of FIJ. The corresponding experiments were conducted on the joint test platform, and experimental results validated the improvements of the proposed control scheme as the dynamical parameters of the FIJ are time-varying and uncertain.

The noise of the torque sensor's output is worse. How to improve the quality of the sensor's output and how to combine the nominal model and MFAC method is the problem we will work on in the near future.

REFERENCES

[1] C. T. Kiang, A. Spowage, and C. K. Yoong, "Review of control and sensor system of flexible manipulator," *J. Intell. Robot. Syst. Theory Appl.*, vol. 77, no. 1, pp. 187–213, 2015.

[2] A. Albu-Schäffer, C. Ott, and G. Hirzinger, "A unified passivity-based control framework for position, torque and impedance control of flexible joint robots," *Int. J. Rob. Res.*, vol. 26, no. 1, pp. 23–39, 2007.

[3] L. M. Sweet and M. C. Good, "Re-definition of the robot control problem," *IEEE Control Syst. Mag.*, pp. 18–25, 1985.

[4] J. B. Mbede and J. J. B. Mvogo Ahanda, "Exponential tracking control using backstepping approach for voltage-based control of a flexible joint electrically driven robot," *J. Robot.*, vol. 2014, 2014.

[5] E. Sariyildiz, G. Chen, and H. Yu, "Robust position control of a novel series elastic actuator via disturbance observer," *2015 IEEE/RSJ Int. Conf. Intell. Robot. Syst.*, pp. 5423–5428, 2015.

[6] J. Montgomery, S. I. Roumeliotis, A. Johnson, and L. Matthies, "Actuator control for the NASA-JSC Valkyrie humanoid robot: A decoupled dynamics approach for torque control of series elastic robots," *J. F. Robot.*, vol. 23, no. 3, pp. 245–267, 2006.

[7] X. Wang, X. Li, J. Wang, X. Fang, and X. Zhu, "Data-driven model-free adaptive sliding mode control for the multi degree-of-freedom robotic exoskeleton," *Inf. Sci. (Ny).*, vol. 327, pp. 246–257, 2016.

[8] L. Li and Z. Z. Mao, "Direct adaptive control for a class of MIMO nonlinear discrete-time systems," *J. Syst. Eng. Electron.*, vol. 25, no. 1, pp. 129–137, 2014.

[9] Z. Hou and S. Jin, "A novel data-driven control approach for a class of discrete-time nonlinear systems," *IEEE Trans. Control Syst. Technol.*, vol. 19, no. 6, pp. 1549–1558, 2011.

[10] A. A. Sinica, "Model-free adaptive control based lateral control of self-driving car," *Acta Autom. Sin.*, vol. 43, no. 11, pp. 1931–1940, 2017.

[11] D. Zhou, D. Sun, Z. Pang, and G. Liu, "Data-based predictive control for networked non-linear systems with two-channel packet dropouts," *IEEE Trans. Ind. Electron,* vol. 9, no. 7, pp. 1154–1161, 2015.

[12] M. W. Spong, "Modeling and control of elastic joint robots," *J. Dyn. Syst. Meas. Control*, vol. 109, no. 4, p. 310, 1987.

[13] S. Chen and S. A. Billingst, "Representations of non-linear systems: The narmax model," *International Journal of Control*, vol. 49, no. 3. pp. 1013–1032, 1989.

[14] X. Bu, F. Yu, Z. Hou, and H. Zhang, "Model-free adaptive control algorithm with data dropout compensation," *Math. Probl. Eng.*, vol. 2012, 2012.

[15] Z. Hou, S. Member, R. Chi, and H. Gao, "An overview of Dynamic-Linearization-based data-driven control and applications," *IEEE Trans. Ind. Electron,* vol. 64, no. 5, pp. 4076–4090, 2017.

[16] Z. Hou and S. Jin, "Model Free Adaptive Control: Theory and Applications," CRC Press, 2013.

[17] J. Pérez, V. Milanés, and E. Onieva, "Cascade architecture for lateral control in autonomous vehicles," *IEEE Trans. Intell. Transp. Syst.*, vol. 12, no. 1, pp. 73–82, 2011.